SUPPLEMENTARY INFORMATION

AXL targeting abrogates autophagic flux and induces immunogenic cell death in drug resistant cancer cells

Lotsberg ML, Wnuk-Lipinska K, Terry S, Tan TZ, Lu N, Trachsel-Moncho L, Røsland GV, Siraji MI, Hellesøy M, Rayford A, Jacobsen K, Ditzel HJ, Vintermyr OK, Bivona TG, Minna J, Brekken RA, Baguley B, Micklem D, Akslen LA, Gausdal G, Simonsen A, Thiery JP, Chouaib S, Lorens JB, Engelsen AST,

AXL targeting abrogates autophagic flux and induces immunogenic cell death in drug resistant cancer cells, Journal of Thoracic Oncology (2020),

doi: https://doi.org/10.1016/ j.jtho.2020.01.015.

Table S1

A

Gene	Fold change (EB/E)	*P* value
KLHL24	-2,7101	3,953E-05
EFNA1	-2,5355	3,362E-05
PDK4	-2,4983	1,406E-06
TXNIP	-2,3464	9,240E-06
HBP1	-2,2778	5,839E-08
PIK3IP1	-2,2154	9,389E-06
FBXO32	-2,1058	7,170E-04
KCNJ13	-1,9786	3,360E-04
BMF	-1,9636	8,424E-04
SNORD3A	-1,8966	1,138E-04
TMEM140	-1,8426	2,078E-03
CDKN1B	-1,8386	4,284E-05
SNORD3C	-1,8171	5,656E-04
SNORD3D	-1,8129	2,385E-04
ELF3	-1,7845	4,775E-05
LFNG	-1,7660	2,774E-05
FRAT2	-1,7344	1,088E-06
HIST2H4A	-1,6569	7,939E-05
C10orf10	-1,6421	3,064E-03
BRD8	-1,6354	1,269E-04
GRB7	-1,6317	6,708E-04
PRR15L	-1,6056	6,645E-04
GBP2	-1,6026	1,438E-04
CCDC28A	-1,5606	4,973E-04
GCNT1	-1,5570	5,532E-03
C5orf41	-1,5358	8,829E-06
TAGLN	-1,5329	8,487E-03
C13orf15	-1,5274	2,328E-03
PMM1	-1,5154	3,137E-03
C17orf44	-1,5073	4,680E-04

Gene	Fold change (EB/E)	*P* value
KCTD6	1,5038	1,750E-05
TUBA4A	1,5238	6,178E-04
CHSY1	1,5242	1,077E-04
CCRN4L	1,5268	7,306E-04
NXT1	1,5312	1,997E-04
PTGS2	1,5348	1,956E-03
CTGF	1,5769	7,102E-05
FOXC1	1,5901	5,908E-04
IL1B	1,5906	2,474E-04
TRPC6	1,5969	6,013E-03
TP63	1,5974	3,733E-04
URB2	1,6088	9,090E-06
PAG1	1,6103	1,668E-03
TNFRSF10A	1,6184	3,697E-04
ADORA2B	1,6294	3,341E-04
KRT16	1,6304	1,735E-03
AMD1	1,6347	2,305E-04
TBX15	1,6444	6,591E-04
CYR61	1,6526	7,775E-03
ARL4C	1,6575	7,909E-06
TRIB1	1,6627	9,010E-05
EDN2	1,6630	2,085E-06
AXUD1	1,6823	4,445E-03
PPRC1	1,7227	1,748E-04
SPRED1	1,7269	5,818E-05
CSF2	1,7350	3,905E-03
HES1	1,7472	1,527E-04
CX3CL1	1,8021	2,309E-03
SLC20A1	1,8139	1,658E-05
ID1	1,8252	8,288E-05
PTHLH	1,8628	2,235E-03
MARS2	1,8871	7,683E-06
SPRY1	1,9047	5,154E-06
MYC	1,9115	2,690E-04
ISG20L1	1,9713	2,218E-04
FOSL1	1,9747	1,906E-05
LOC729252	1,9796	9,626E-05
HBEGF	2,0086	1,762E-03
SPRY2	2,0291	6,845E-06
FGFBP1	2,0312	6,696E-04
EPHA2	2,1752	1,718E-05
LOC730525	2,1834	2,605E-05
C8orf4	2,2129	1,130E-03
ANGPTL4	2,2148	1,882E-03
FAM46C	2,2319	6,557E-03
DUSP5	2,3142	6,464E-07
SPRY4	2,3600	8,543E-06
HAS3	2,3973	7,051E-04
HSPA1A	2,3979	2,966E-04
ERRFI1	2,4286	1,043E-04
PHLDA1	2,5452	5,304E-05
FOXQ1	2,6982	3,320E-05
BHLHB2	2,7663	1,649E-04
EGR1	2,8068	3,171E-05
MGC102966	3,0360	9,450E-05
LOC400578	3,1101	1,026E-04
IER3	3,2548	5,301E-05
DUSP6	5,5468	8,772E-08

B

Gene ontology (GO) biological process complete	Expected	Fold Enrich.	Significance (*P*)
neutrophil chemotaxis	.28	21.71	3.49E-03
negative regulation of MAP kinase activity	.32	21.56	3.81E-04
response to gamma radiation	.24	21.11	3.83E-02
regulation of ERK1 and ERK2 cascade	1.13	9.72	1.74E-04
regulation of angiogenesis	.99	9.12	6.09E-03
regulation of cysteine-type endopeptidase activity involved in apoptotic process	.89	8.98	2.89E-02
aging	1.32	8.33	8.16E-04
response to lipopolysaccharide	1.43	7.67	1.85E-03
positive regulation of response to external stimulus	1.18	7.60	2.68E-02
inflammatory response	2.11	7.57	3.03E-06
response to hypoxia	1.40	7.17	1.24E-02
cellular response to growth factor stimulus	2.07	6.76	1.72E-04
regulation of sequence-specific DNA binding transcription factor activity	1.65	6.67	7.22E-03
blood vessel morphogenesis	1.67	6.58	8.20E-03
morphogenesis of an epithelium	1.84	6.51	2.84E-03
MAPK cascade	1.63	6.14	4.79E-02
positive regulation of cell migration	1.80	6.12	1.66E-02
reproductive structure development	1.86	5.91	2.28E-02
positive regulation of apoptotic process	2.59	5.80	3.83E-04

Table S2

A

Target	Product Number	Supplier	Dilution (Application)	Host Species
Apoptosis cocktail: actin, caspase 3, PARP	ab136812	Abcam	1:250 (WB)	Rabbit/ Mouse
AXL	1H12-1B7-5D6	BerGenBio	1:1000 (WB)	Mouse
AXL	MAB154	R&D Systems	1:100 (Flow)	Mouse
Beclin-1	3495	Cell Signaling Tech.	1:1000 (WB)	Rabbit
Beta-actin	ab8227	Abcam	1:1000 (WB)	Rabbit
Calreticulin	ab83220	Abcam	1:100 (Flow)	Rabbit
Cleaved caspase 3	9661	Cell Signaling Tech.	1:500 (WB)	Rabbit
Cleaved caspase 8	9496	Cell Signaling Tech.	1:1000 (WB)	Rabbit
E-cadherin	14472S	Cell Signaling Tech.	1:1000 (WB) 1:100 (ICC)	Mouse
GAPDH	ab128915	Abcam	1:50,000 (WB)	Rabbit
LC3A/B (D3U4C)	12741	Cell Signaling Tech.	1:1000 (WB) 1:100 (ICC)	Rabbit
N-cadherin	ab18203	Abcam	1:500 (WB)	Rabbit
pAkt (Ser473)	9271	Cell Signaling Tech.	1:1000 (WB)	Rabbit
pAXL (Tyr779)	AF2228	R&D Systems	1 µg/ml (WB)	Rabbit
SQSTM1/p62	ab56416	Abcam	1:1000 (WB)	Mouse
Vimentin	ab92547	Abcam	1:5000 (WB) 1:100 (ICC)	Rabbit

B

Antibody target	Clone	Metal tag	Conc./Dilution	Product number / Supplier
Cleaved caspase 3	5A1E (cleaved at Asp175)	142 Nd	1 µg/ml	9661, CST
pStat3	4 (pY705)	145 Nd	4 µg/ml	612356, BD
pStat5	47 (pY694)	146 Nd	2 µg/ml	61964, BD
PD-L1	29E.2A3	148 Nd	1:50	3148017B, Fluidigm
pEGFR	Y38 (pTyr1068)	149 Sm	0.5 µg/ml	ab5644, Abcam
pRb	J112-906 (pSer807/811)	150 Nd	1:200	201313, Fluidigm
pAkt	D9E (pS473)	152 Sm	1:50	3152005A, Fluidigm
pStat1	4a (pY701)	153 Eu	1:50	3153005A, Fluidigm
Vimentin	D21H3	154 Sm	4 µg/ml	5741, CST
p38	D3F9	156 Gd	1:50	3156002A, Fluidigm
E-cadherin	24E11	158 Gd	1:200	3158021A, Fluidigm
pMAPKAPK2	27B7	159 Tb	1:50	3158021A, Fluidigm
pErk1/2	20A (pT202/pY204)	161 Gd	1 µg/ml	612358, BD
pPLCg2	K86-689.37 (pY759)	162 Dy	2 µg/ml	558490, BD
TGFβ	TW46H10	163 Dy	1:200	3163010B, Fluidigm
pNFκB	K10-895.12.50 (pS529)	166 Er	0.5 µg/ml	558393, BD
YAP	H9 (C-terminal 379-407)	167 Er	1 µg/ml	sc-271134, Santa Cruz
Axl	1H12 (total)	168 Er	2 µg/ml	BerGenBio
EGFR	AY13	170 Er	1:400	3170009B, Fluidigm
pS6	N7-548 (pS235/S236)	172 Yb	1:200	3172008A, Fluidigm
pHistone H3	HTA28 (pSer28)	175 Lu	1:200	201313, Fluidigm
CD44	IM7 (total, surface)	176 Yb	0.125 µg/ml	553131, BD

Figure S1

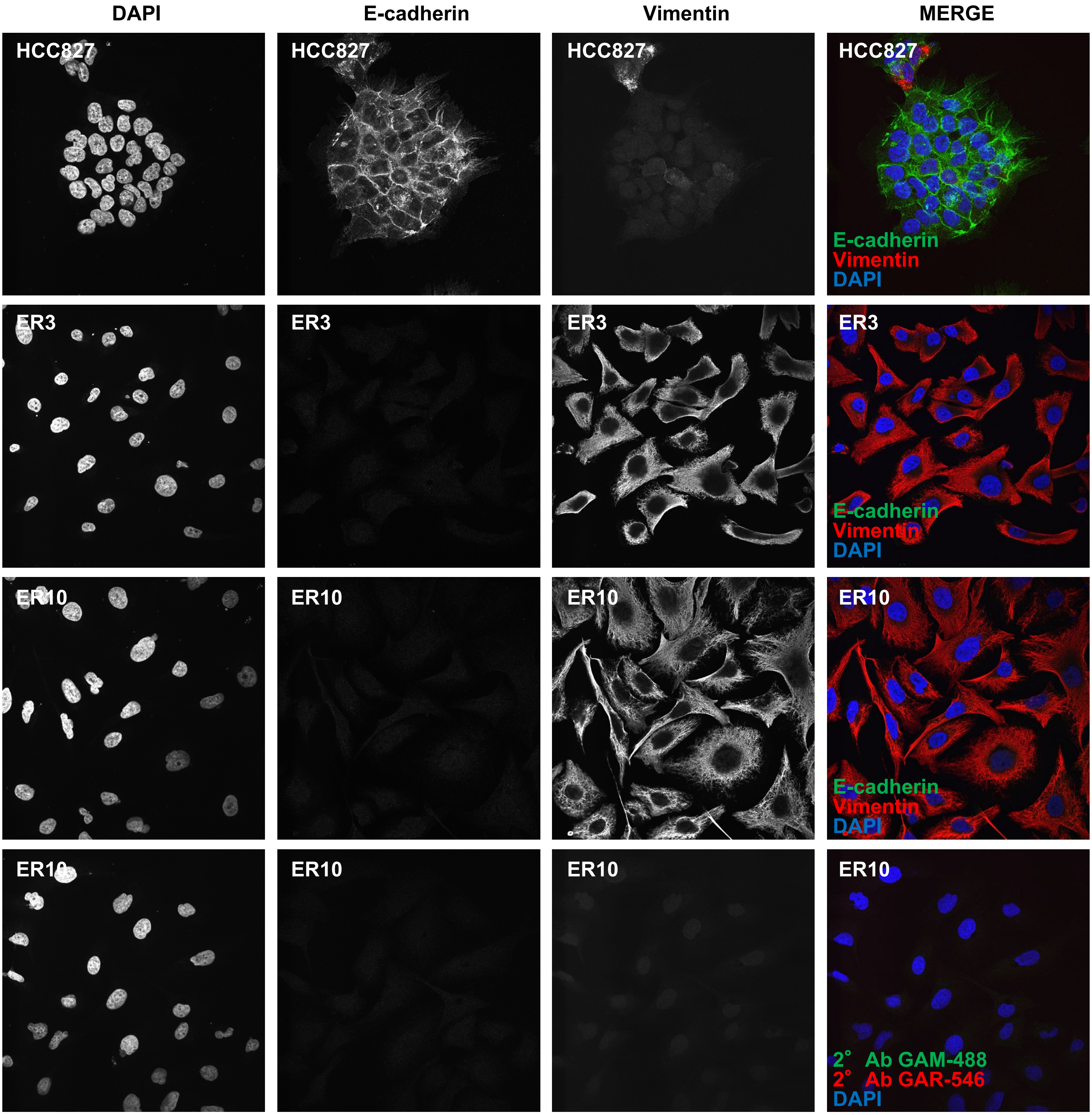
DAPI
E-cadherin
Vimentin
MERGE
HCC827
HCC827
HCC827
HCC827
E-cadherin
Vimentin
DAPI
ER3
ER3
ER3
ER3
E-cadherin
Vimentin
DAPI
ER10
ER10
ER10
ER10
E-cadherin
Vimentin
DAPI
ER10
ER10
ER10
ER10
2° Ab GAM-488
2° Ab GAR-546
DAPI

Figure S2

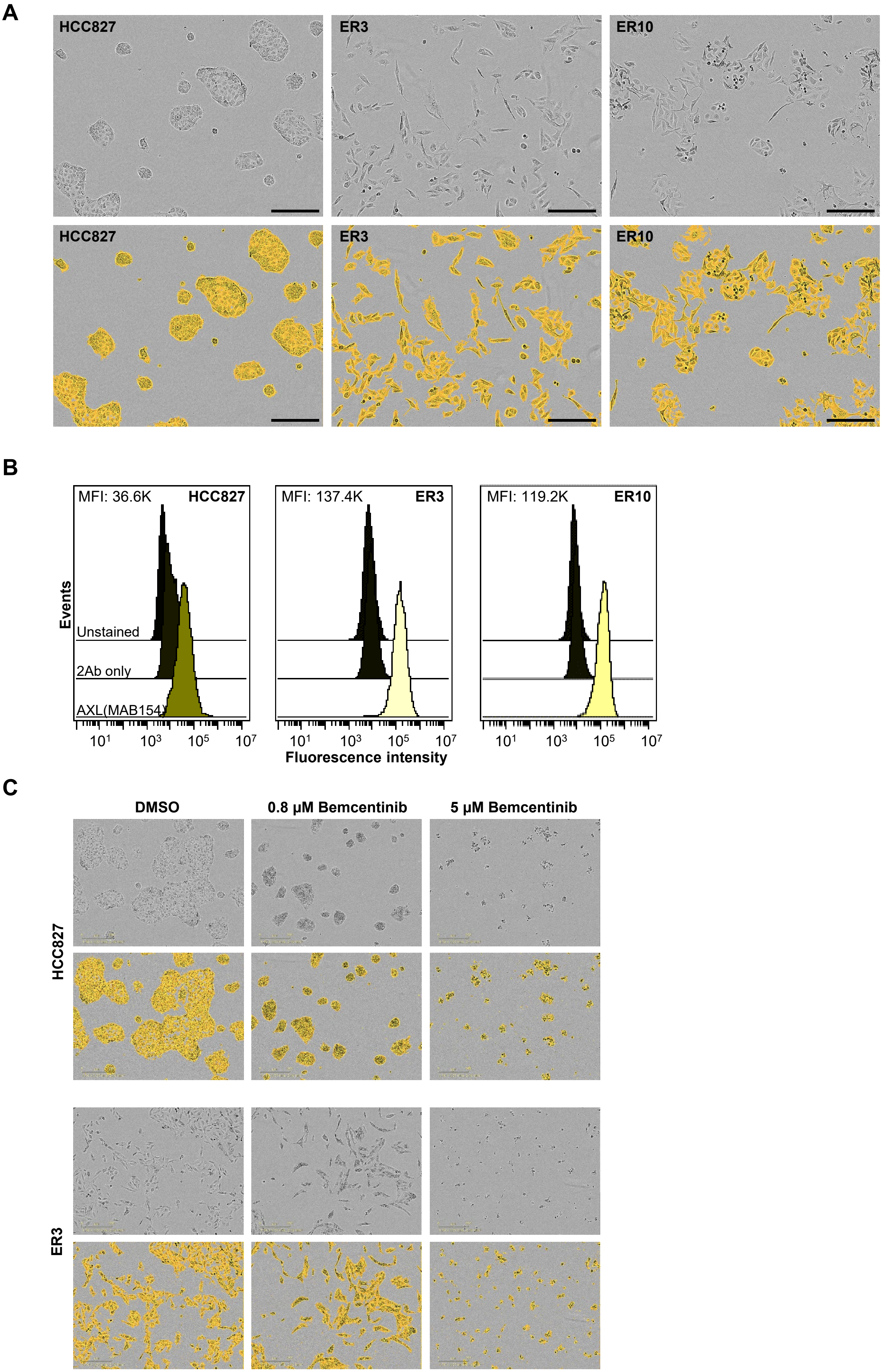
A
HCC827
ER3
ER10
HCC827
ER3
ER10
B
MFI: 36.6K
HCC827
MFI: 137.4K
ER3
MFI: 119.2K
ER10
Events
Unstained
2Ab only
AXL(MAB154)
10^1
10^3
10^5
10^7
Fluorescence intensity
C
DMSO
0.8 µM Bemcentinib
5 µM Bemcentinib
HCC827
ER3

Figure S3

A

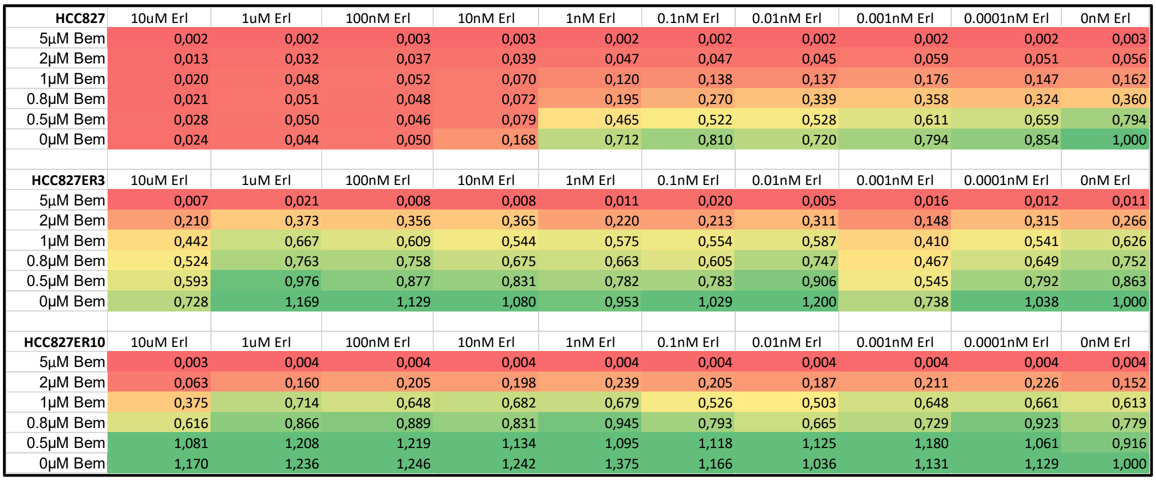

Cell viability

HCC827	10uM Erl	1uM Erl	100nM Erl	10nM Erl	1nM Erl	0.1nM Erl	0.01nM Erl	0.001nM Erl	0.0001nM Erl	0nM Erl
5µM Bem	0,002	0,002	0,003	0,003	0,002	0,002	0,002	0,002	0,002	0,003
2µM Bem	0,013	0,032	0,037	0,039	0,047	0,047	0,045	0,059	0,051	0,056
1µM Bem	0,020	0,048	0,052	0,070	0,120	0,138	0,137	0,176	0,147	0,162
0.8µM Bem	0,021	0,051	0,048	0,072	0,195	0,270	0,339	0,358	0,324	0,360
0.5µM Bem	0,028	0,050	0,046	0,079	0,465	0,522	0,528	0,611	0,659	0,794
0µM Bem	0,024	0,044	0,050	0,168	0,712	0,810	0,720	0,794	0,854	1,000

HCC827ER3	10uM Erl	1uM Erl	100nM Erl	10nM Erl	1nM Erl	0.1nM Erl	0.01nM Erl	0.001nM Erl	0.0001nM Erl	0nM Erl
5µM Bem	0,007	0,021	0,008	0,008	0,011	0,020	0,005	0,016	0,012	0,011
2µM Bem	0,210	0,373	0,356	0,365	0,220	0,213	0,311	0,148	0,315	0,266
1µM Bem	0,442	0,667	0,609	0,544	0,575	0,554	0,587	0,410	0,541	0,626
0.8µM Bem	0,524	0,763	0,758	0,675	0,663	0,605	0,747	0,467	0,649	0,752
0.5µM Bem	0,593	0,976	0,877	0,831	0,782	0,783	0,906	0,545	0,792	0,863
0µM Bem	0,728	1,169	1,129	1,080	0,953	1,029	1,200	0,738	1,038	1,000

HCC827ER10	10uM Erl	1uM Erl	100nM Erl	10nM Erl	1nM Erl	0.1nM Erl	0.01nM Erl	0.001nM Erl	0.0001nM Erl	0nM Erl
5µM Bem	0,003	0,004	0,004	0,004	0,004	0,004	0,004	0,004	0,004	0,004
2µM Bem	0,063	0,160	0,205	0,198	0,239	0,205	0,187	0,211	0,226	0,152
1µM Bem	0,375	0,714	0,648	0,682	0,679	0,526	0,503	0,648	0,661	0,613
0.8µM Bem	0,616	0,866	0,889	0,831	0,945	0,793	0,665	0,729	0,923	0,779
0.5µM Bem	1,081	1,208	1,219	1,134	1,095	1,118	1,125	1,180	1,061	0,916
0µM Bem	1,170	1,236	1,246	1,242	1,375	1,166	1,036	1,131	1,129	1,000

B

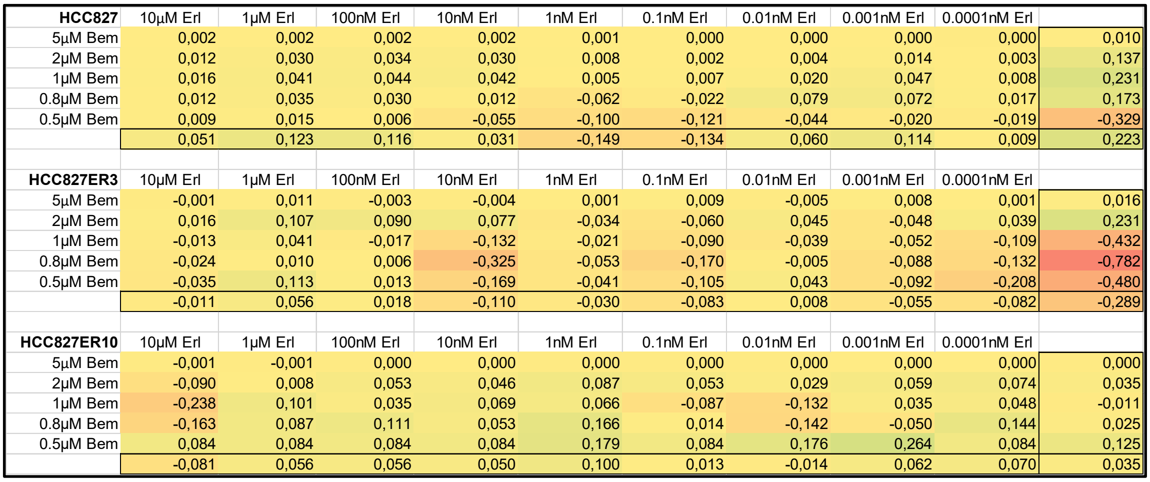

Delta Bliss

HCC827	10µM Erl	1µM Erl	100nM Erl	10nM Erl	1nM Erl	0.1nM Erl	0.01nM Erl	0.001nM Erl	0.0001nM Erl	
5µM Bem	0,002	0,002	0,002	0,002	0,001	0,000	0,000	0,000	0,000	0,010
2µM Bem	0,012	0,030	0,034	0,030	0,008	0,002	0,004	0,014	0,003	0,137
1µM Bem	0,016	0,041	0,044	0,042	0,005	0,007	0,020	0,047	0,008	0,231
0.8µM Bem	0,012	0,035	0,030	0,012	-0,062	-0,022	0,079	0,072	0,017	0,173
0.5µM Bem	0,009	0,015	0,006	-0,055	-0,100	-0,121	-0,044	-0,020	-0,019	-0,329
	0,051	0,123	0,116	0,031	-0,149	-0,134	0,060	0,114	0,009	0,223

HCC827ER3	10µM Erl	1µM Erl	100nM Erl	10nM Erl	1nM Erl	0.1nM Erl	0.01nM Erl	0.001nM Erl	0.0001nM Erl	
5µM Bem	-0,001	0,011	-0,003	-0,004	0,001	0,009	-0,005	0,008	0,001	0,016
2µM Bem	0,016	0,107	0,090	0,077	-0,034	-0,060	0,045	-0,048	0,039	0,231
1µM Bem	-0,013	0,041	-0,017	-0,132	-0,021	-0,090	-0,039	-0,052	-0,109	-0,432
0.8µM Bem	-0,024	0,010	0,006	-0,325	-0,053	-0,170	-0,005	-0,088	-0,132	-0,782
0.5µM Bem	-0,035	0,113	0,013	-0,169	-0,041	-0,105	0,043	-0,092	-0,208	-0,480
	-0,011	0,056	0,018	-0,110	-0,030	-0,083	0,008	-0,055	-0,082	-0,289

HCC827ER10	10µM Erl	1µM Erl	100nM Erl	10nM Erl	1nM Erl	0.1nM Erl	0.01nM Erl	0.001nM Erl	0.0001nM Erl	
5µM Bem	-0,001	-0,001	0,000	0,000	0,000	0,000	0,000	0,000	0,000	0,000
2µM Bem	-0,090	0,008	0,053	0,046	0,087	0,053	0,029	0,059	0,074	0,035
1µM Bem	-0,238	0,101	0,035	0,069	0,066	-0,087	-0,132	0,035	0,048	-0,011
0.8µM Bem	-0,163	0,087	0,111	0,053	0,166	0,014	-0,142	-0,050	0,144	0,025
0.5µM Bem	0,084	0,084	0,084	0,084	0,179	0,084	0,176	0,264	0,084	0,125
	-0,081	0,056	0,056	0,050	0,100	0,013	-0,014	0,062	0,070	0,035

C

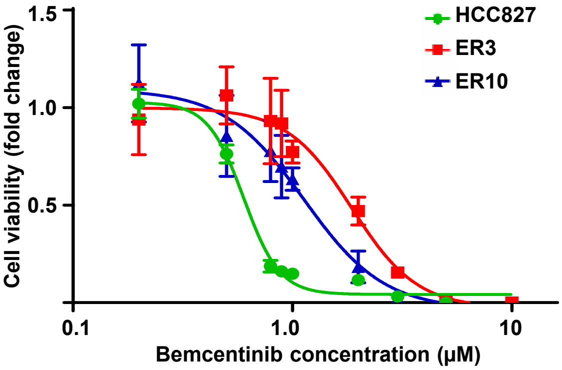

D

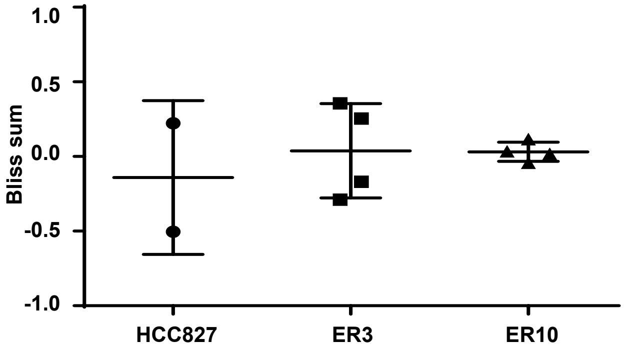

E

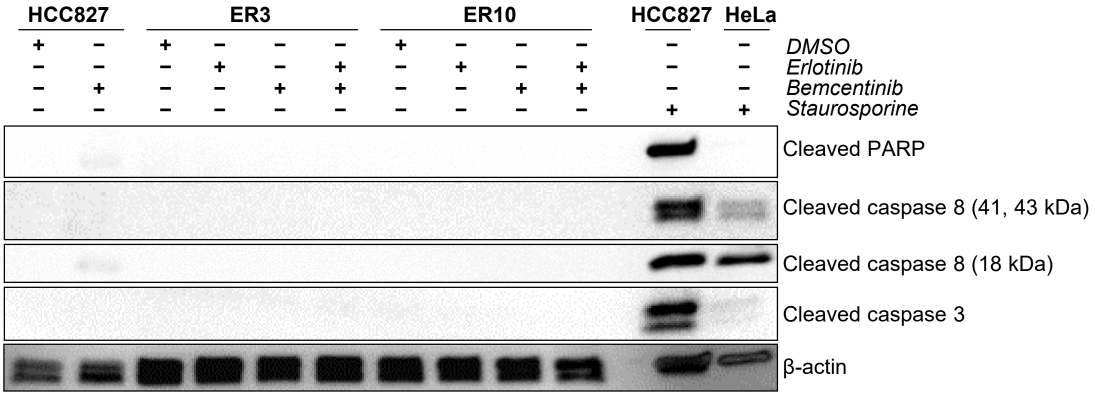

Figure S4

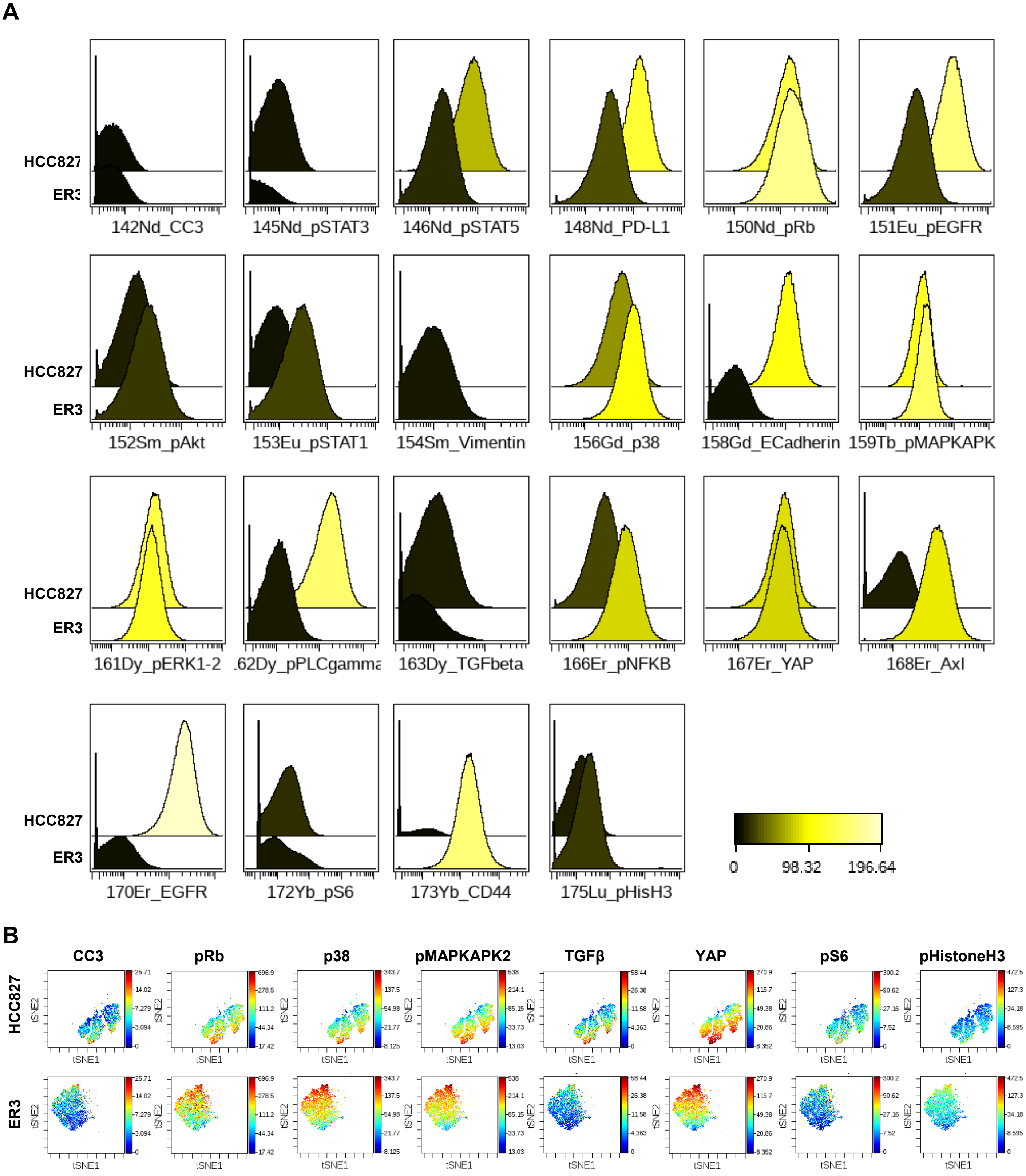

C

	142Nd_CC3	145Nd_pSTAT3	146Nd_pSTAT5	148Nd_PDL1	150Nd_pRb	151Eu_pEGFR	152Sm_pAkt	153Eu_pSTAT1	154Sm_Vimentin	156Gd_p38	158Gd_ECadherin	159Tb_pMAPKAPK2	161Dy_pERK12	162Dy_pPLCgamma2	163Dy_TGFbeta	166Er_pNFKB	167Er_YAP	168Er_Axl	170Er_EGFR	172Yb_pS6	173Yb_CD44	175Lu_pHisH3
HCC827	4.53	7.95	71.24	123.79	136.08	160.7	12.29	7.23	0.0	56.82	105.54	113.92	135.17	151.98	10.51	26.96	85.89	11.31	196.64	17.7	3.97	12.0
ER3	4.01	2.95	16.20	30.24	167.72	27.15	21.3	25.17	8.99	103.44	6.82	146.81	115.1	9.93	4.99	83.02	82.12	90.68	6.35	9.06	157.37	21.89

Figure S5

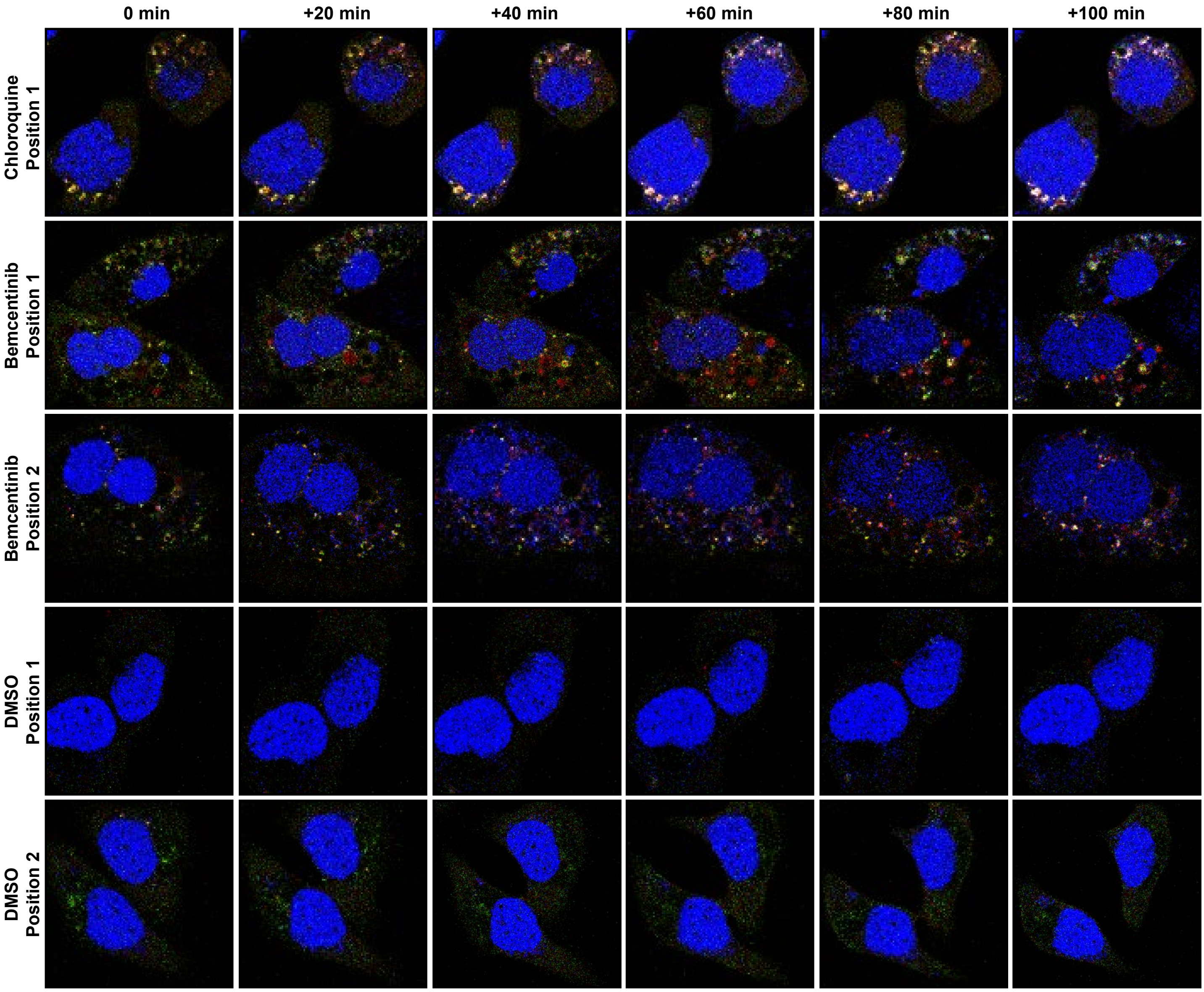
0 min
+20 min
+40 min
+60 min
+80 min
+100 min
Chloroquine Position 1
Bemcentinib Position 1
Bemcentinib Position 2
DMSO Position 1
DMSO Position 2

Figure S6

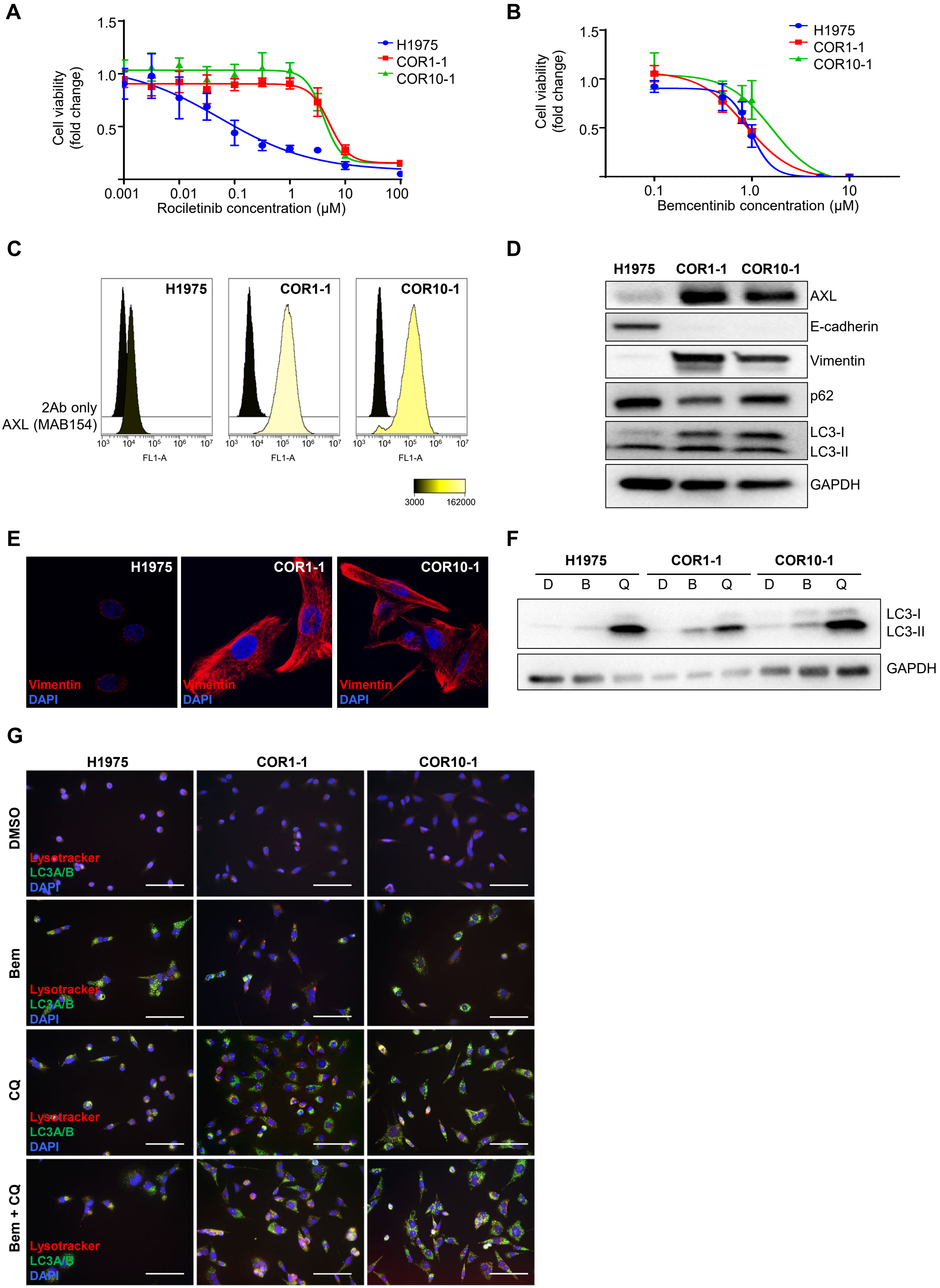
A
Cell viability (fold change)
1.5
1.0
0.5
0.001
0.01
0.1
1
10
100
Rociletinib concentration (μM)
H1975
COR1-1
COR10-1
B
Cell viability (fold change)
1.5
1.0
0.5
0.1
1.0
10
Bemcentinib concentration (μM)
H1975
COR1-1
COR10-1
C
H1975
COR1-1
COR10-1
2Ab only
AXL (MAB154)
10³
10⁴
10⁵
10⁶
10⁷
FL1-A
3000
162000
D
H1975
COR1-1
COR10-1
AXL
E-cadherin
Vimentin
p62
LC3-I
LC3-II
GAPDH
E
H1975
COR1-1
COR10-1
Vimentin
DAPI
F
H1975
COR1-1
COR10-1
D
B
Q
LC3-I
LC3-II
GAPDH
G
H1975
COR1-1
COR10-1
DMSO
Bem
CQ
Bem + CQ
Lysotracker
LC3A/B
DAPI

SUPPLEMENTARY FIGURE LEGENDS

Table S1. Genes differentially expressed between erlotinib/bemcentinib -treated and erlotinib-monotherapy treated HCC827 parental tumors

(A) Nude mice challenged with 8 million HCC827 cells were treated with 50 mg/kg of bemcentinib, *b.i.d.*, and 50 mg/kg of erlotinib, *q.d.* and euthanized after 25 days of treatment. Gene expression analysis of mRNA extracts was performed using the Illumina Human HT-12 v4 Expression BeadChip whole-genome expression array. Probe level and gene level data were imported into J-Express Pro and differentially expressed genes between erlotinib-bemcentinib combinational treatment and erlotinib monotherapy-treated tumors were identified by the significance analysis of microarray (SAM). Differentially expressed genes (cutoff: 1.5-fold change and $p < 0.01$) are listed. **(B)** Gene ontology (GO) analysis of upregulated genes in erlotinib- and bemcentinib-treated versus erlotinib-treated tumors. The table displays fold enrichment and p values, sorted by fold enrichment with the most specific biological process in the hierarchy displayed. Fold enrichment is calculated as the number of genes found in the gene list above (cutoff: 1.5-fold change and $p < 0.01$) with a certain GO term divided by the number of genes expected (based on the size of the list and number of genes in genome within the GO term). A Bonferroni correction for multiple testing was applied.

Table S2. List of antibodies

(A) Summary of antibodies used for western blot, flow cytometry and ICC. **(B)** Antibody target, clone and phospho-epitope, metal tag, final concentration or dilution, as well as product-number and supplier are given for each antibody included in the mass cytometry time of flight (CyTOF) experiment.

Figure S1. Immunofluorescence: single channel display and negative control

Single channel displays and secondary antibody only negative control for the images shown in Figure 2B. Scale bar: 50 μm.

Figure S2. IncuCyte Live Cell Imaging and AXL Flow Cytometry

(A) Brightfield images obtained by IncuCyte ZOOM system without (upper row) and with (lower row) cell mask generated by the IncuCyte ZOOM software reveal the morphology and growth pattern of the parental HCC827 cells, ER3, and ER10 clones. Scalebar: 300 μm **(B)** Representative flow cytometry histograms of HCC827, ER3, and ER10 cells immunofluorescently stained for AXL (n = 3 independent experiments). MFI = median fluorescence intensity. **(C)** Brightfield images obtained by IncuCyte ZOOM system without (upper row) and with (lower row) cell mask generated by the IncuCyte ZOOM software reveal the cellular morphology and growth pattern of the parental HCC827 and ER3 cells following 48 h bemcentinib treatment as indicated.

Figure S3. Drug response to erlotinib and the selective AXL inhibitor bemcentinib in erlotinib-sensitive versus erlotinib resistant cells

(A) Heat map of cell viability followed by 5 days treatment with erlotinib ± bemcentinib at indicated concentrations used for delta Bliss analysis. Values ranging from 0 (red) to 1 (green) represent the mean of two independent experiments of n = 6 replicates/sample. Normalization was performed against the vehicle (DMSO)-treated sample for each cell line. **(B)** Synergy between erlotinib and bemcentinib was evaluated by the delta Bliss independence model. **(C)** The sensitivity of HCC827, ER3, and ER10 cells to the selective small molecule AXL inhibitor bemcentinib was measured by reszasurin assay following 5 days treatment, and the IC50 values for HCC827 cells was 0.664 μM ± 0.065, and 1.119 μM ± 0.110 for ER3, and 1.198 μM ± 0.115 for ER10 (mean IC50 value ± SEM, for n = 4-6 independent experiments). **(D)** Delta Bliss values calculated from the n = 2-4 independent experiments. **(E)** Western blots to evaluate the induction of apoptosis in HCC827, ER3, and ER10 cells treated with erlotinib (1 μM) and bemcentinib (0.8 μM) for 24 hours. HCC827 and HeLa cells treated with staurosporine (1 μM) were included as positive controls. Western blots for cleaved PARP (89 kDa), cleaved caspase 8 (43, 41, and 18 kDa), cleaved caspase 3 (19, 17 kDa) are shown. β-actin (42 kDa) is shown as a loading control.

Figure S4. Additional CyTOF results

(A) Histogram representation of the intensities of the 22 markers in the CyTOF panel. HCC827 parental cells (upper histogram), ER3 (lower histogram). Number of ion-clouds representing single cells on the y-axis. **(B)** viSNE plots displaying additional markers from the CyTOF panel. **(C)** Table summarizing median intensity values for all channels.

Figure S5. Live cell time lapse of the autophagic flux

ER10 cells stably expressing mCherry-EGFP-LC3B protein were pretreated with chloroquine (50 μM), bemcentinib (0.8 μM) or vehicle control (DMSO), for 24 hours and imaged by Leica SP8 confocal microscopy every 10 minutes over a time course of 100 minutes. Images from 1-2 representative positions are shown for each condition. The counterstain was performed with the nuclear dye Draq5 (blue).

Figure S6. Characterization of H1975 cells and rociletinib resistant clones

(A) Sensitivity to rociletinib (CO-1686) in H1975, COR1-1 and COR10-1 cells measured by resazurin cell viability assay after 5 days treatment. **(B)** Sensitivity to bemcentinib in H1975 COR1-

1 and COR10-1 cells measured by resazurin cell viability assay after 5 days treatment. **(C)** Representative flow cytometry histograms of HCC827, ER3, and ER10 cells immunofluorescently stained for AXL by MAB154 antibody reveal single-cell level of AXL expression (n = 3 independent experiments). Y-axis represents the number of cells, and color intensity represents the fluorescence intensity. **(D)** Western blot for H1975, COR1-1, COR10-1 cell lysates for immunodetection of AXL (144kDa), E-cadherin (CDH1, 135 kDa), vimentin (VIM, 54 kDa), p62 (SQSTM, 62 kDa) and LC3A/B (LC3-I 17 kDa, LC3-II 19 kDa). GAPDH is shown as a loading control. **(E)** Representative confocal images of H1975, COR1-1 and COR10-1 cells immunofluorescently labelled for the mesenchymal intermediate filament vimentin (VIM, red); DAPI nuclear stain (blue). **(F)** Western blotting shows relative protein levels of LC3A/B (LC3-I 17 kDa, LC3-II 19 kDa) in lysates of H1975, COR 1-1, and COR10-1 cells treated for 24 hours by vehicle (DMSO; D), bemcentinib (0.8 μM; B) or chloroquine (50 μM; Q). GAPDH (37 kDa) is shown as a loading control. **(G)** Staining of the erlotinib resistant H1975 parental cells and the rocletinib resistant clones COR1-1 and COR10-1 by LysoTracker (red DN-99) in combination with anti-LC3A/B antibody reveals the presence of lysosomes (red puncta), autophagosomes (green puncta), and autolysosomes (yellow puncta) in cells treated with vehicle (DMSO), bemcentinib (0.8 μM), chloroquine (50 μM), or bemcentinib (0.8 μM) in combination with chloroquine (50 μM) for 24 hours. Scale bar: 100 μm.